Design of the Helix–Turn–Helix Motif: Nonlocal Effects of Quaternary Structure in DNA Recognition Investigated by Laser Raman Spectroscopy†

James M. Benevides,‡ Michael A. Weiss,§ and George J. Thomas, Jr.*,‡

Division of Cell Biology and Biophysics, School of Basic Life Sciences, University of Missouri—Kansas City, Kansas City, Missouri 64110, and Department of Biological Chemistry and Molecular Pharmacology, Harvard Medical School, Boston, Massachusetts 02115

Received December 12, 1990; Revised Manuscript Received February 15, 1991

ABSTRACT: The operator-binding domain of phage λ repressor provides a model for DNA recognition by the helix–turn–helix (HTH) motif. In the wild-type protein, dimerization is mediated by hydrophobic packing (of the dyad-related helix 5), which serves as an indirect determinant of operator affinity. The mutant repressor, Tyr88 → Cys, forms an intersubunit disulfide linkage and exhibits enhancement of both structural stability and operator affinity. Yet the dimer-specific operator affinity of the mutant is 10-fold weaker than that of the wild-type (noncovalent) dimer, suggesting nonlocal effects of the intersubunit disulfide bond on HTH recognition (Sauer et al., 1986). To explore such nonlocal effects, we describe laser Raman studies of the Cys88 mutant repressor and its interaction with operator sites O_L1 and O_R3. The following results have been obtained: (i) Wild-type and mutant dimers exhibit similar secondary structures, indicated by quantitative comparison of Raman amide I and amide III bands. (ii) The engineered disulfide of the mutant lacks rigorous symmetry; we observe mainly the gauche/gauche/trans CC–S–S–CC rotamer. (iii) Remarkably, distinctive local and nonlocal differences are observed in the mechanisms of DNA recognition by wild-type and mutant repressors. These differences involve specific hydrogen-bonding interactions between the protein and DNA, including guanine N7 sites in the major groove of DNA, and alterations in DNA phosphodiester conformation induced by protein binding. We analyze these differences in relation to crystal structures of the wild-type dimer with and without bound DNA. The crystal structures are notable for large-scale changes in subunit orientation upon DNA binding and suggest that corresponding motions may be constrained in the covalent dimer. Our results emphasize the role of induced fit in protein–DNA recognition.

The N-terminal domain of the λ repressor has been extensively investigated as a helix–turn–helix (HTH) protein and a model for protein folding and design (Hochschild et al., 1983; Hecht et al., 1983; Sauer et al., 1986; Lim & Sauer, 1989). Pabo and colleagues determined the structure of the N-terminal domain in two crystal forms: with and without specifically bound operator DNA (Pabo & Lewis, 1982; Jordan & Pabo, 1988). These and related crystallographic studies of phage 434 repressors (Aggarwal et al., 1988; Wolberger et al., 1988; Mondragon et al., 1989a,b) have provided a detailed view of the HTH motif as a scaffold for DNA recognition (Harrison & Aggarwal, 1990). We previously described laser Raman studies of the λ repressor as a foundation for the application of vibrational spectroscopy to protein–DNA recognition (Thomas et al., 1986). This approach was recently extended in studies of sequence-dependent changes in DNA structure induced by binding of a repressor to specific operators (Benevides et al., 1991). In the present work, we examine the role of protein flexibility in DNA recognition. Comparative Raman studies of the wild-type repressor and an engineered variant suggest that changes in quaternary structure are required for formation of the specific repressor–operator complex.

The N-terminal domain (residues 1–102) forms a stable dimer in the absence of DNA (Weiss et al., 1987a,b) and also binds specifically as a dimer to the λ operator, retaining the regulatory properties of the intact protein (Sauer et al., 1979,1986; Jordan & Pabo, 1988). The dimer contact is formed by interaction between symmetry-related helices (helix 5), while the HTH motif comprises helices 2 and 3 with an intervening turn, as shown in Figure 1 (Pabo & Lewis, 1982). The interface of the wild-type protein dimer contains symmetry-related tyrosines (Y88 and Y88′) that are positioned close to the dyad axis and together with neighboring hydrophobic sites provide a functional dimer contact (Pabo & Lewis, 1982; Reidhaar-Olson & Sauer, 1988). As a specific example of altering the functional properties of a protein by mutagenesis, Pabo and Suchanek (1986) proposed that introduction of an intersubunit disulfide bridge to form a covalent dimer would enhance operator affinity of the repressor N-terminal domain. The engineered protein (Y88 → C) was constructed and observed to form a stable C88–C88′ bridge (Sauer et al., 1986). The resulting covalent dimer in fact exhibited a 10-fold increase in apparent operator affinity relative to the monomeric wild-type N-terminal repressor fragment. Nevertheless, the *dimer-specific* affinity of the engineered protein was observed to be reduced 10-fold relative to that calculated for the preformed wild-type dimer (Sauer et al., 1986). This discrepancy suggested structural differences between the covalent dimer and the DNA-bound conformation of the wild-type protein. The X-ray structure of the wild-type repressor–operator complex has been determined (Jordan & Pabo, 1988) and

† Paper XLI in the series Raman Spectral Studies of Nucleic Acids. Supported by grants from the National Institutes of Health to G.J.T. (AI11855 and AI18758) and M.A.W. (HD26465). M.A.W. is supported in part by the Pfizer Scholars Program for New Faculty and an American Cancer Society Junior Faculty Research Award.

* To whom correspondence should be addressed.
‡ University of Missouri—Kansas City.
§ Harvard Medical School.

0006-2960/91/0430-4381$02.50/0

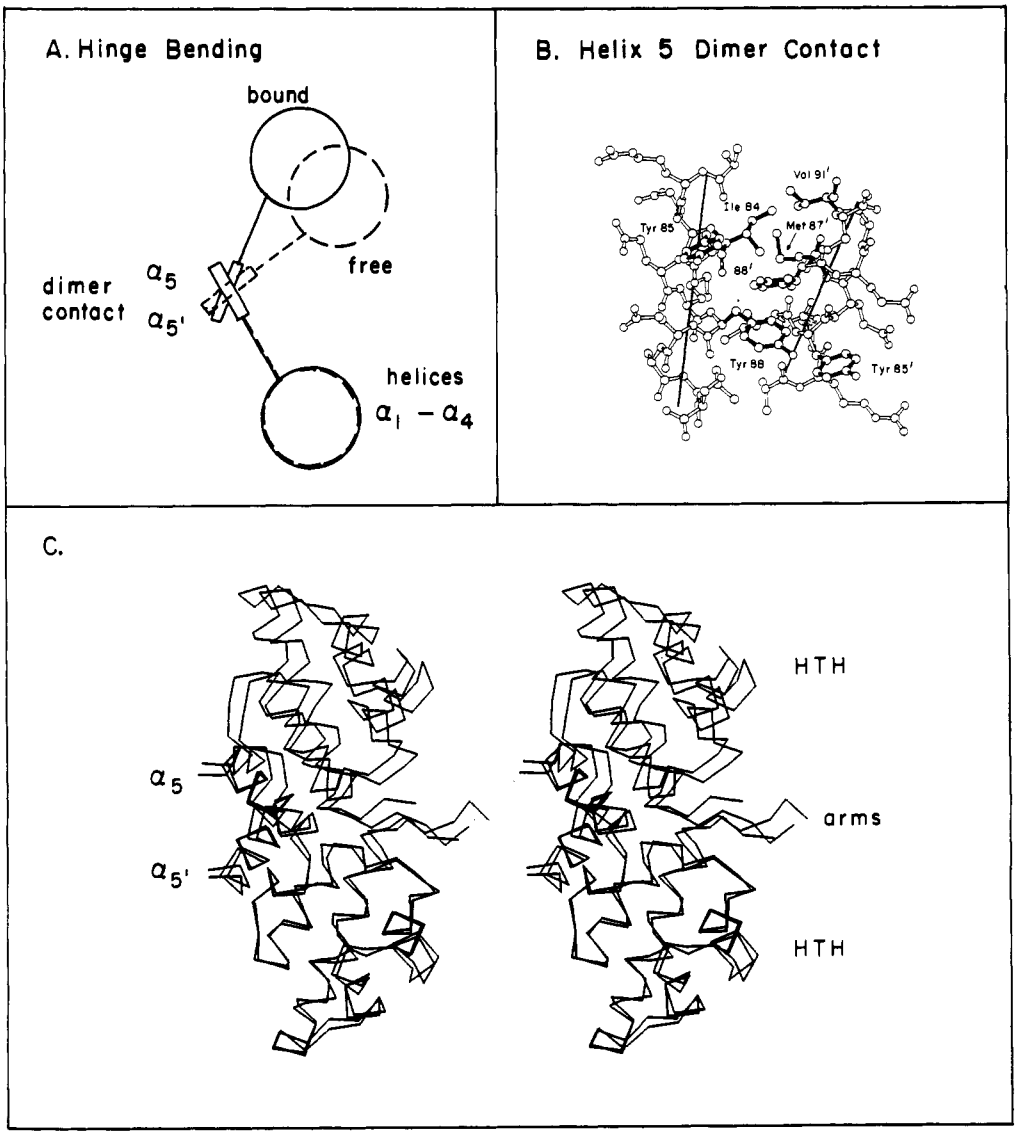

FIGURE 1: Illustrations of the helix–turn–helix domain of the λ repressor. (A) Schematic representation of hinge-bending motion in the λ repressor (side view) as inferred from the crystal structures of the free protein (Pabo & Lewis, 1982) and the specifically bound protein–DNA complex (Jordan & Pabo, 1988). For clarity, the degree of relative subunit rotation is accentuated in the drawing; the actual value is approximately 5° (see panel C). The four helices comprising the globular portion of the domain are labeled α_1–α_4; the fifth helix (α_5) forms the dimer contact. (B) Ball-and-stick model of the dimer contact (back view), which is formed by the hydrophobic packing of dyad-related amphipathic helices (helices 5 and 5′). The internal residues are shown by solid lines. These include Val91, Tyr88, Met87, and Ile84. Tyr88 packs against Tyr88′; the corresponding Cys88 side chains form a stable intermolecular disulfide bridge in an engineered protein (Sauer et al., 1986). The axes of the two helices are indicated by solid lines. For clarity, the view has been rotated from the center of approximate symmetry. (C) Superposition (side view) of the crystal structures of free (residues 4–92; Pabo & Lewis, 1982) and DNA-bound N-terminal domains (residues 1–92; Jordan & Pabo, 1988). The lower protomers were aligned in the two structures to minimize the root-mean-square displacement of backbone atoms. In this alignment the upper protomers undergo a relative rigid-body rotation of approximately 5°. The two helix–turn–helix units are labeled HTH; the N-terminal arms are indicated. Residues 1–3 are not visualized in the crystal structure of the free domain and accordingly are not shown.

provides a basis for the present Raman study. The crystal structures of the Y88C mutant and its DNA complex have not been determined.

The N-terminal domain of the λ repressor provides a convenient model system in which to investigate how engineered changes in subunit orientation influence protein–DNA contacts at a distance. To what extent are changes in protein quaternary structure linked to protein–DNA recognition, and how may this be affected by an intersubunit disulfide bond? As a first step toward answering these questions we have undertaken comparative laser Raman studies of the wild-type and mutant (Y88C) repressor–operator complexes. In the absence of DNA, the wild-type and mutant domains are similar, in accord with previous model-building (Pabo & Suchanek, 1986) and ^{1}H NMR studies (Sauer et al., 1986; Weiss et al., 1987a,b). Remarkably, however, the wild-type and mutant repressors exhibit different modes of DNA binding. These results suggest that the engineered disulfide constrains the induced fit between the λ repressor and operator, leading to loss of specific interactions involving amino acid side chains and DNA functional groups of the specific complex. A similar (but more marked) change in subunit orientation is observed in the λ Cro–operator complex (Brennan et al., 1990), suggesting that our results may reflect a general feature of protein–DNA recognition.

Materials and Methods

Protein Purification. The wild-type and Y88C mutant fragments (residues 1–102) of the λ repressor were purified from overproducing strains of *Escherichia coli* as described (Sauer et al., 1986). Operator DNA sites O_L1 and O_R3 were synthesized and prepared as described (Benevides et al., 1991).

Preparation of Repressor-Operator Complexes. Repressor–operator complexes were prepared by dissolving the appropriate weight of the operator (O_L1 or O_R3) in a solution containing 50 mg/mL repressor. Complexes containing 1:1 and 2:1 molar ratios of repressor monomer to operator duplex were investigated. The 1:1 ratio provides a solution in which virtually all the repressor is bound to DNA but contains an approximate 0.5-fold molar excess of protein-free DNA. The 2:1 ratio at equilibrium contains predominantly (>90%) complexed material.

Raman Spectroscopy. Solutions were sealed in glass capillary cells (Kimax #34507) that were thermostated at 12 °C in the sample illuminator of the spectrometer while Raman spectra were recorded. For operators, repressors, and their complexes, spectra were obtained over the interval 300–1800 cm^{-1}. All spectra were excited with the 514.5-nm line of a Coherent Innova 70 argon laser and were recorded on a Spex Ramalog V/VI spectrometer under the control of an IBM-XT microcomputer. Data were collected at increments of 1 cm^{-1} with an integration time of 1.5 s and spectral slit width of 8 cm^{-1} or less. Raman spectra collected over extended intervals (300–1800 or 600–1800 cm^{-1}), and displayed in the illustrations are the unsmoothed averages of eight to ten scans of 1.5-cm^{-1} or better repeatability. Additional signal averaging was employed for scans over narrower spectral intervals, such as those emcompassing disulfide stretching (300–625 cm^{-1}), amide III (1200–1400 cm^{-1}) and amide I (1500–1800 cm^{-1}) bands. In all cases, the scattering by the aqueous solvent was compensated by use of computer subtraction techniques described previously (Benevides et al., 1984). The Raman frequencies reported for discrete peaks in the spectra are accurate to within ±2 cm^{-1}.

We have employed the following criteria for discussion of features in the difference spectra. First, a difference band is deemed of significant intensity if it reflects *both* a signal-to-noise ratio of at least 2:1 in the difference spectrum computed from signal-averaged minuend and subtrahend spectra *and* a relative intensity change of at least 10% in its parent bands. Second, the difference band must be structurally interpretable. Thus, while a difference band may in principle be significant by the first criterion, it may be impossible to interpret in sufficient detail to warrant discussion. In fact there are few examples of bands in the present spectra that meet only the first criterion.

Results

Our results are presented in two parts. The Raman spectra of the wild-type and Y88C mutant repressor domains are compared in the first part. Whereas no major differences are observed in the predominantly α-helical protein secondary structure, the mutation is shown to generate nonlocal changes in configurations of multiple side chains. The wild-type and mutant protein–DNA complexes are described in the second part. Remarkably, these complexes exhibit distinguishable features, suggesting significant differences in local and overall aspects of the protein–DNA interface. The results are analyzed in the discussion, in reference to the crystal structures of the N-terminal domain (Pabo & Lewis, 1982) and its specific DNA complex (Jordan & Pabo, 1988).

Raman Spectra of Wild-Type and Mutant Repressors

Backbone Vibrations. Raman spectra of the wild-type repressor fragment (designated RF) and the Y88 → C mutant (designated C88RF) and their corresponding difference spectrum (mutant minus wild-type) are shown in Figure 2 for the region 600–1800 cm^{-1}. The Raman spectrum of the

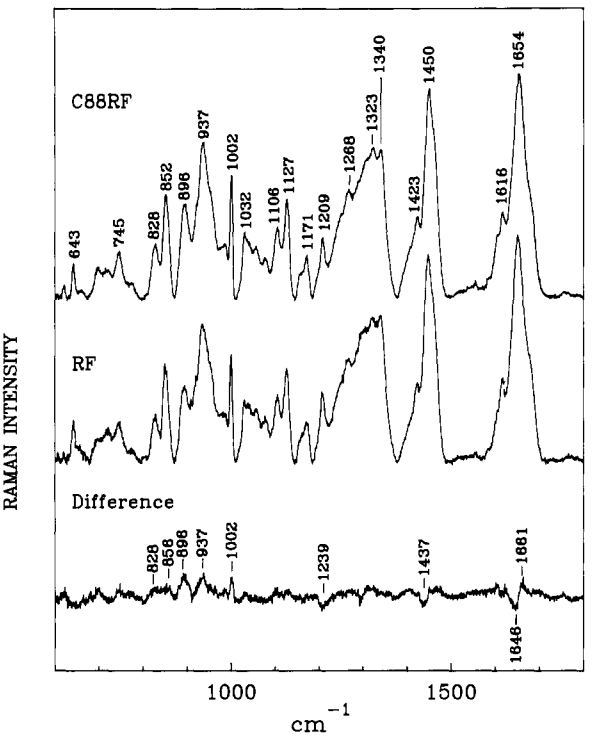

FIGURE 2: Raman spectra in the region 600–1800 cm^{-1} of the wild-type repressor fragment (RF) and the Y88C mutant (C88RF) and their corresponding difference spectrum (computed as C88RF minus RF). Conditions: Protein concentration = 100 mg/mL in 10 mM tris, pH 7.5; excitation wavelength = 514.5 nm; slit width = 8 cm^{-1}. Data are averages of 10 scans, corrected for buffer as described (Benevides et al., 1991), and normalized to give the same integrated amide I intensities.

mutant protein is very similar to that previously assigned for the wild-type protein (Thomas et al., 1986), indicating similar secondary structures. Only weak bands are present in the difference spectrum of Figure 2, as next discussed.

For both RF and C88RF, the intense amide I bands are centered near 1650 cm^{-1} and the prominent amide III shoulders near 1280–1300 cm^{-1}. These bands indicate predominantly α-helical secondary structure (Thomas et al., 1986). The intense skeletal N–C–Cα–Cβ mode near 937 cm^{-1} (Krimm, 1987) is also indicative of the very high α-helical secondary structure in both the wild-type and mutant proteins. The absence of intense Raman bands diagnostic of an altered or significantly perturbed peptide backbone in the mutant fragment is consistent with its ^1H NMR features and thermal stability (Sauer et al., 1986). This result is also in accord with the predictions of protein design (Pabo & Suchanek, 1986). We note particularly the absence of significant difference bands throughout the amide III region (1240–1300 cm^{-1}) and only a relatively minor difference feature in the amide I region, consisting of a possible shift of about 3% of the amide I peak from ca. 1650 cm^{-1} to slightly higher frequency ca. 1660 cm^{-1}. (The latter features may include contributions from imperfectly compensated solvent in one or both spectra. Nevertheless, even if attributed entirely to amide I, these results show that at least 96% of the wild-type secondary structure is preserved in the mutant, i.e., a difference of at most three helical residues).

Side-Chain Vibrations. The wild-type and mutant proteins exhibit more significant intensity differences in several Raman bands of the 500–1100 cm^{-1} interval, as labeled in Figure 2. For example, the difference peaks near 828 (Y), 856 (Y), 937 (coupled N–C–Cα–Cβ stretching), and 1002 cm^{-1} (F) represent substantial percent changes in the intensities of the

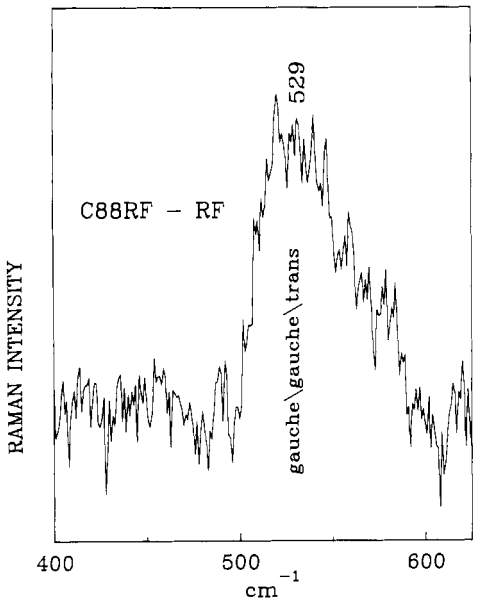

FIGURE 3: Raman difference spectrum between wild-type and mutant repressor fragments (C88RF minus RF) in the region 400–625 cm^{-1}, showing the disulfide stretching band of C88RF at 529 cm^{-1}, which is assigned mainly to the gauche/gauche/trans (CC–S–S–CC) rotamer. The other conditions are as given in Figure 2.

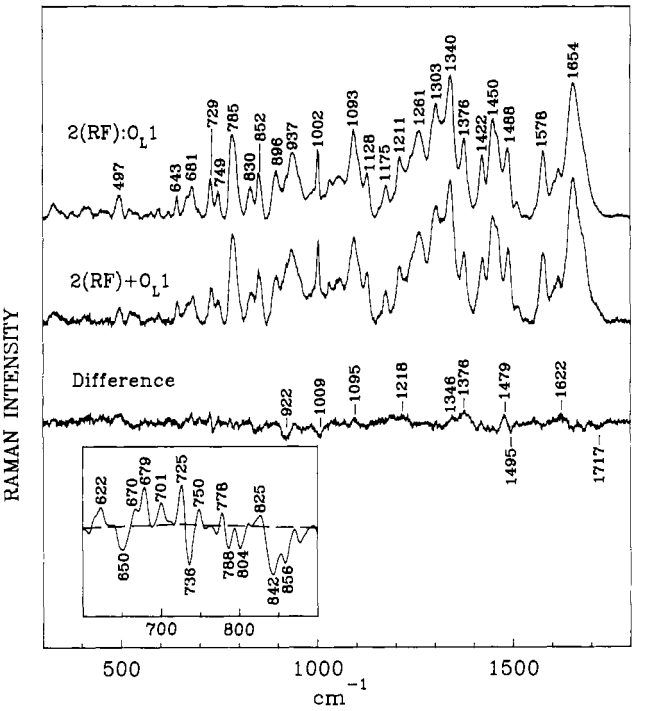

FIGURE 4: Raman spectum in the region 300–1800 cm^{-1} of the 2:1 complex of wild-type repressor with O_L1 [2(RF):O_L1, top], the sum of constituents [2(RF) + O_L1, middle), and corresponding difference (complex minus sum, bottom). The inset shows a 5-fold amplification of the difference in the region of DNA backbone markers discussed in the text.

parent bands. The first three of these differences are as expected for the Y88C substitution and relate directly to tyrosine- and cystine-specific vibrational modes (Thomas et al., 1986). Band intensity changes of phenylalanine or other side chains presumably reflect nonlocal effects of the mutation. Tyrosine, cystine, and nonlocal vibrational modes are discussed in turn below.

Tyrosine Fermi Doublet. The data of Figure 2 allow us to measure with greater precision than previously (Thomas et al., 1986) the intensity ratio I_{856}/I_{828} of tyrosine bands in RF and C88RF. This intensity ratio indicates the distribution of phenolic OH groups among hydrogen-bond acceptor (A), donor (D), and simultaneous acceptor/donor (E) states (Siamwiza et al., 1975). For RF we obtain I_{856}/I_{828} = 2.05, indicating 3A + 2E tyrosines in the wild-type dimer; for C88RF, we obtain I_{856}/I_{828} = 1.88, indicating 2A + 2E in the covalent dimer and therefore identifying Y88 as a tyrosine of type A, *i.e., the phenolic OH group of Y88 accepts, but does not donate, a hydrogen bond.* The remaining tyrosines of the RF dimer are confirmed as listed previously in Table III of Thomas et al. (1986), i.e., Y22 (A), Y60 (E), Y85 (A), Y88 (A), and Y101 (E).

Disulfide Stretching Modes. Figure 3 shows amplification of the difference spectrum (C88RF minus RF) in the region of 400–625 cm^{-1}. These data reveal a positive band centered near 529 cm^{-1} that is assignable to the S–S stretching vibration of the C88RF dimer. Previous studies of model compounds show that the Raman disulfide stretching band is a sensitive indicator of disulfide bridge conformation: The S–S stretching band is expected at 510 ± 5, 525 ± 5, or 540 ± 5 cm^{-1}, respectively, for gauche/gauche/gauche (g/g/g); gauche/gauche/trans (g/g/t), or trans/gauche/trans (t/g/t) rotamers of the Cα–Cβ–S–S–Cβ′–Cα′ network (Sugeta et al., 1973). The location of the peak of the Raman disulfide band close to 525 cm^{-1} in C88RF (Figure 3) thus identifies the g/g/t rotamer as the most populated Cα–Cβ–S–S–Cβ′–Cα′ conformation. Since the band is relatively broad (half width ≈ 50 cm^{-1}), substantial populations may also exist for g/g/g and t/g/t rotamers. Interestingly, despite the identical protomer sequences in this symmetric dimer, the CC–S–S–CC networks do not uniformly assume symmetrical configurations.

Nonlocal Side-Chain Vibrations. The aforementioned CC–S–S–CC configuration suggests that the mutant (covalent) dimer and wild-type (noncovalent) dimer may not have identical subunit interfaces. This could result from differences in side-chain packing in the two dimer structures. As shown above, such differences do not significantly alter either the percentage of subunit α-helix or the overall secondary structures of the subunits. Therefore, the appearance of a small but signifcant difference band in Figure 2 near 937 cm^{-1} indicates that RF and C88RF, despite identical secondary structures, do not have identical configurations for all N–C–Cα–Cβ linkages. Evidently, differences occur between the wild-type and mutant repressors in (a small number of) Cα–Cβ conformations. Although the Raman spectra do not provide a quantitative indication of the number of side chains affected, this difference may significantly influence the DNA-binding characteristics of the two proteins, as next discussed.

Raman Spectra of Repressor–Operator Complexes

The Raman spectrum in the 300–1800 cm^{-1} region of the 2:1 complex of the wild-type repressor fragment and O_L1 [designated 2(RF):O_L1] is shown in Figure 4. The spectrum of the specific complex (top trace) differs from the sum of spectra of constituents (middle trace) as indicated by the difference spectrum (bottom trace). The difference bands reveal perturbations primarily to the DNA conformation as a result of repressor binding (DNA bands at 650, 679, 725–736, 842, 1095, 1218, 1346, 1376, 1479–1495, and 1622 cm^{-1}). Changes in Raman bands assigned to specific side chains of the repressor are also observed in the difference spectrum (RF bands at 922 and 1009 cm^{-1}). These changes have been interpreted and discussed in detail in the following paper of this series (Benevides et al., 1991).

Corresponding spectra of the specific 2:1 complex of C88RF and O_L1 [designated 2(C88RF):O_L1] are shown in Figure 5.

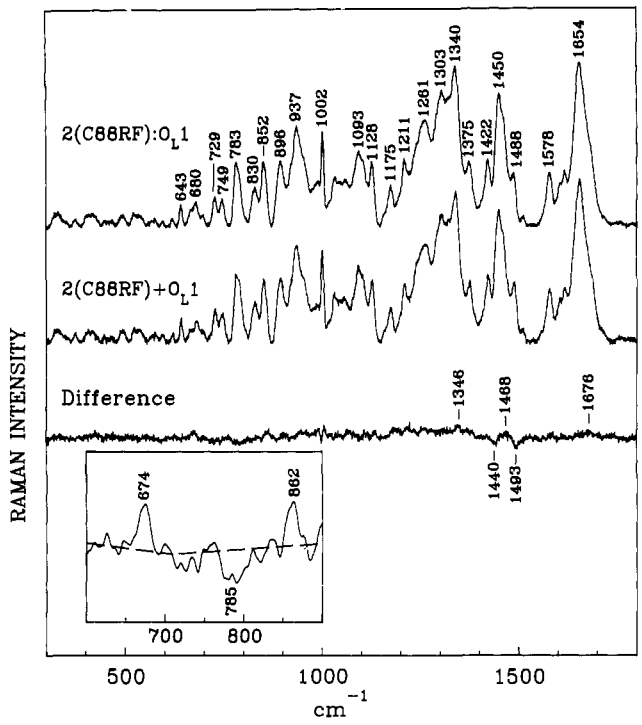

FIGURE 5: Raman spectrum in the region 300–1800 cm^{-1} of the 2:1 complex of mutant repressor with O_L1 [2(C88RF):O_L1, top], the sum of constituents [2(C88RF) + O_L1, middle], and corresponding difference (complex minus sum, bottom). The inset shows a 5-fold amplification of the difference spectrum in the region of DNA backbone markers.

Comparison of the difference spectra of the wild-type (Figure 4) and mutant (Figure 5) complexes indicates few shared features. Clearly, the two difference spectra are significantly different from one another. They exhibit fundamentally different peaks and troughs, indicating that wild-type and mutant repressors form distinguishable complexes with O_L1. The distinctive DNA-specific and protein-specific difference bands are next discussed in turn.

DNA Backbone Vibrations. The difference spectrum of the 2(RF):O_L1 complex (Figure 4, inset) is remarkable for its negative band near 842 cm^{-1}, indicating that O–P–O torsions at several AT pairs are altered with RF binding. The 2(RF):O_L1 complex also exhibits positive difference intensity at 622, 670, 679, 701, 725, and 750 cm^{-1} and negative intensity at 650, 736, and 788 cm^{-1}. These perturbations have been discussed (Benevides et al., 1991) and indicate that dA and dT nucleoside conformations [Table I of Benevides et al. (1991)] are the more significantly altered by RF binding. These results are in accord with crystallographic observations that the AT-rich ends of the wild-type repressor-bound operator differ from canonical B-DNA more significantly than does the central GC-rich domain (Jordan & Pabo, 1988). Strikingly, the 2(C88RF):O_L1 complex exhibits its largest difference bands (Figure 5, inset) at positions corresponding to GC markers. No prominent difference signals are observed near 840 cm^{-1} that could be attributed to a structural change at AT base-pairs for the mutant repressor complex.

DNA Pyrimidine-Specific Vibrations. Methylation of the pyrimidine 5C site generates an intense Raman band at 1376 cm^{-1} (Benevides et al., 1984). Since in the repressor–operator complexes there is little overlap of the 1376-cm^{-1} band with bands from the protein, differences in the band profile can be assigned with confidence to changes in the thymine methyl group environment. The difference spectra of Figures 4 and 5 show that the 1376-cm^{-1} band exhibits increased intensity in each complex relative to the corresponding unbound operator. We suggest that this intensity increase is associated with the shielding of thymine methyl groups from their usual environment in the major groove by bound repressor and that this feature is similar in the wild-type and mutant complexes. Jordan and Pabo (1988) have proposed that hydrophobic pockets are formed along the repressor–operator interface to shield from solvent the methyl groups of thymines T3 and T13′ of the consensus half-site (and presumably also T13 of the nonconsensus half-site).

DNA Purine-Specific Vibrations. In guanine mononucleotides and in B-DNA, the guanine ring generates an intense band near 1490 cm^{-1} (Lord & Thomas, 1967; Small & Peticolas, 1971). This band shifts to 1480 cm^{-1} when N7 accepts a strong hydrogen bond (as in Hoogsteen complexes) or is coordinated to divalent metal ions (Hartman et al., 1973; Nishimura et al., 1986). Both the 2(RF):O_L1 and 2(C88RF):O_L1 complexes exhibit a shift of Raman intensity from 1490 to 1480 cm^{-1} with complex formation, providing direct evidence of hydrogen-bond formation between repressor side chains and guanine N7 sites in the major groove. The magnitude of the intensity shift, corresponding to the involvement of at least two guanines, is similar in the 2(RF):O_L1 and 2(C88RF):O_L1 complexes. [The procedure for estimating the minimum number of interacting guanine residues from this measurement is discussed in the subsequent paper of this series (Benevides et al., 1991).]

The difference spectrum of the wild-type O_L1 complex exhibits a negative band at 1717 cm^{-1} (Figure 4), which is attributed to the effect of guanine 6C=O interactions with repressor residues (Prescott et al., 1984; Benevides et al., 1988). Such hydrogen bonding is expected to alter the Raman C=O band profile in the 1650–1750-cm^{-1} region (Bellamy, 1980). A 1717-cm^{-1} band is not observed in the difference spectrum of the mutant complex (Figure 5), suggesting that the guanine 6C=O acceptors do not interact in the same way with the mutant repressor. The sites of such 6C=O hydrogen-bonding interactions observed in the wild-type cocrystal structure involve the interaction of G14′ and G12′ with O–H of Ser45 and N–H of Lys4, respectively (Jordan & Pabo, 1988). Since these residues are distant from the site of mutation (C88), the Raman data indicate nonlocal changes in the architecture of the protein–DNA complex.

Protein Backbone Vibrations. Neither the wild-type nor the mutant complex exhibits difference bands in the amide I and amide III regions. These data indicate that no significant change in protein secondary structure occurs upon DNA binding (within the ±3% limits of precision of the present Raman measurements). This finding for the solution structures is in accord with crystal structures of the native domain in the presence and absence of DNA (Pabo & Lewis, 1982; Jordan & Pabo, 1988).

Protein Side-Chain Vibrations. The Raman intensity ratio I_{856}/I_{828} is diagnostic of the net hydrogen-bonding environment of repressor tyrosines (Y22, Y60, Y85, Y88, and Y101) (Thomas et al., 1986). As discussed elsewhere (Benevides et al., 1991), perturbation of this doublet ratio is observed in the wild-type fragment upon DNA binding. This perturbation if ascribed solely to a change in state of one tyrosine per subunit, would correspond to the transfer of that tyrosine from the role of exclusive hydrogen-bond acceptor (A state) to that of both hydrogen-bond donor and acceptor (E state). On the basis of the cocrystal structure of the wild-type 2(RF):O_L1 complex, we have proposed that this tyrosine is Y22 (Benevides et al., 1991). In the cocrystal, the phenolic OH group of Y22 appears to donate a hydrogen bond to the phosphate oxygen of thymine

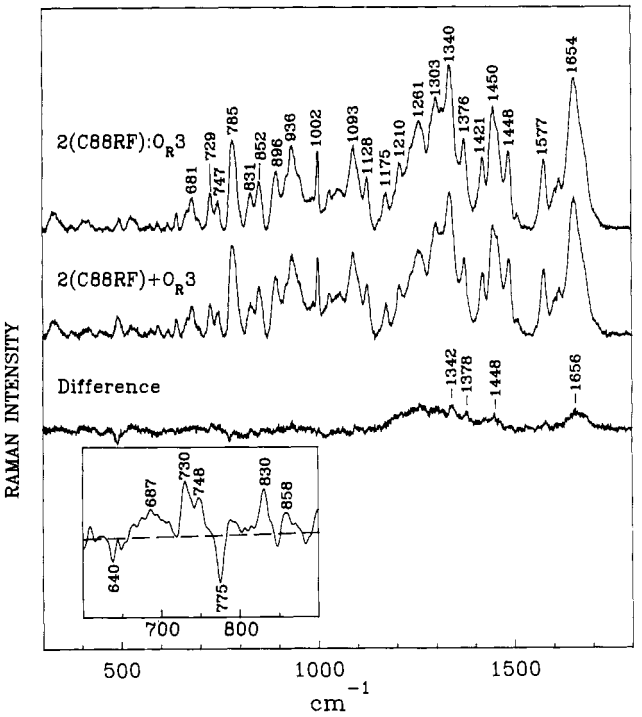

FIGURE 6: Raman spectrum in the region 300–1800 cm^{-1} of the 2:1 complex of mutant repressor with O_R3 [2(C88RF):O_R3, top], the sum of constituents [2(C88RF) + O_R3, middle], and their corresponding difference spectrum (complex minus sum, bottom). The inset shows a 5-fold amplification of the difference spectrum in the region of DNA backbone markers discussed in the text.

residue T1 [designated "phosphate A1" in the notation of Jordan and Pabo (1988)]. In the absence of DNA, the phenolic OH group of Y22 functions exclusively as an acceptor (Thomas et al., 1986). Notably, no net change in the tyrosine doublet ratio is observed for the O_L1 complex of the mutant fragment. This result further indicates the nonlocal nature of changes induced in the mutant complex and may account in part for the observed reduction in dimer-specific operator affinity (Sauer et al., 1986).

Additional difference intensities assignable to Raman bands of amino acid side chains are observed, principally involving bands near 925 (Cα–Cβ stretching of various aliphatic side chains) and 1000 cm^{-1} (Phe aromatic ring). Although specific structural interpretation is not possible, the configurations of many residues are altered by complex formation, and these alterations exhibit marked differences in the wild-type and mutant complexes.

Sequence-Dependent DNA Perturbations. In a related study (Benevides et al., 1991), it is shown that changes in DNA conformation accompany repressor binding and that these changes depend in detail on the sequence (O_L1 or O_R3) of the operator site. We extend these observations by comparison of the spectra of C88RF complexes with O_L1 or O_R3. As shown in Figure 6, corresponding differences are observed in the spectrum of the 2(C88RF):O_R3 complex relative to the 2(C88RF):O_L1 complex. These results are in accord with cocrystal studies of homologous phage repressors by Harrison and Aggarwal (1990). In each case, the precise DNA configuration observed in the crystal is determined by protein binding.

The 2(C88RF):O_R3 complex (Figure 6) exhibits broad positive difference profiles in the regions 1180–1480 cm^{-1} and 1600–1700 cm^{-1}, which encompass the intervals of amide III and amide I bands, respectively. However, discrete peaks assignable to Raman amide bands are not apparent. These features are likely to reflect imperfect matching of baselines in spectra of the complex and constituents, rather than significant structural perturbations.

Discussion

Laser Raman spectroscopy provides a complement to X-ray diffraction and high-resolution NMR methods for the structural analysis of nucleic acids and their complexes. Raman spectra of oligonucleotide crystals have been obtained as a reference data base, permitting empiric classification of perturbations in DNA structure upon protein binding (Benevides et al., 1984, 1986, 1988) [for a review, see Thomas and Wang (1988)]. Such an analysis of sequence-dependent variations in the structure of two λ operator sites upon repressor binding has recently been described (Benevides et al., 1991). Raman spectroscopy also provides information regarding the backbone conformations of proteins and the interactions of selected side chains [for reviews, see Spiro (1987)]. The backbone and side-chain Raman bands of the N-terminal domain of λ repressor were characterized previously (Thomas et al., 1986), providing a foundation for the present analysis of a mutant repressor containing an engineered intersubunit disulfide bond.

The isolated N-terminal domain (residues 1–102) binds as a dimer to operator DNA (Sauer et al., 1979, 1986; Jordan & Pabo, 1988). In this paper we have analyzed nonlocal structural perturbations in the repressor–operator complex resulting from a change in the geometry of the dimer contact. This contact is formed by the interaction of symmetry-related helices (helix 5) and determines the relative orientation of the two HTH surfaces (Figure 1). Interestingly, the opening angle between protomers differs in the structure of the protein alone (Pabo & Lewis, 1982) relative to the protein–DNA complex (Jordan & Pabo, 1988). This difference arises from the rigid rotation of one subunit by approximately 5° about the dyad axis (D. T. Nguyen, M. A. Weiss, and M. Karplus, manuscript in preparation). Rotation in the protein–DNA complex is accomplished by adjustment in multiple side-chain configurations in one protomer to yield an asymmetric dimer. These changes occur primarily in the loop between the dimer contact and the globular region of the repressor. Such angular displacement ($\Delta\Theta$) induces nonlocal changes in side-chain positions ($r\Delta\Theta$) of up to 5 Å between corresponding side chains in the free and DNA-bound repressor. Similar differences in relative subunit orientation have been observed in the crystal structures of the *E. coli* cyclicAMP-activating protein (CAP) and its DNA complex (Steitz, 1990) and in the λ Cro repressor upon operator binding (Brennan et al., 1990). Subunit orientation in CAP appears to be under allosteric regulation by cAMP, which binds at the subunit interface and contacts both protomers at a site distant from the helix–turn–helix motif.

Design of an engineered repressor domain as a covalent dimer was originally described by Pabo and Suchanek (1986) and constructed by Sauer et al. (1986). The dimer-related cysteines are observed to form a stable C88–C88′ bridge, and the resulting dimer exhibits a 10-fold increase in apparent operator affinity (relative to the wild-type noncovalent dimer). Nevertheless, the *dimer-specific* affinity of the engineered protein was reduced 10-fold relative to that calculated for the preformed wild-type dimer (Sauer et al., 1986), suggesting structural differences between the covalent dimer and the DNA-bound conformation of the wild-type protein. Biophysical evidence for nonlocal perturbations in the Y88C domain has previously been described in ^{1}H NMR studies (Sauer et al., 1986; Weiss et al., 1987a,b). Perturbations are observed in the chemical shifts of Y22, F51, and F76; these residues project into the interior of each protomer (helices 1–4; Pabo

& Lewis, 1982). The observed changes in chemical shift are unlikely to be due to ring-current effects associated with removal of the aromatic ring, since corresponding changes in chemical shift do not accompany the monomer–dimer transition in the wild-type fragment, a process that stabilizes the configuration of Y88 (Weiss et al., 1986). Nor are similar changes in chemical shift observed for a monomeric derivative of C88 obtained by acetylation of the thiol (M. A. Weiss, unpublished results). Further, ^{1}H NMR resonances assigned to residues of the loop between helix 4 and helix 5 are broadened by intermediate exchange. These loop residues are observed to be in different local environments in the two crystal structures (Pabo & Lewis, 1982; Jordan & Pabo, 1988), and their NMR exchange features suggest that hinge-bending motions are present in solution (Weiss et al., 1987a; M. A. Weiss, unpublished results). The structure of the C88 domain has not been determined at this time by either NMR or crystallographic methods.

In this paper we have described laser Raman spectroscopic studies of the wild-type and Y88C mutant repressors and their respective operator complexes. These experiments were designed to test for the presence of nonlocal perturbations in the mutant domain. We observed that in the absence of DNA the wild-type and mutant domains exhibit similar secondary structures. Nevertheless, changes occur in multiple side-chain configurations; these changes include at least one phenylalanine, in accord with the pattern of nonlocal ^{1}H NMR perturbations (Weiss et al., 1987a,b) and structural differences between crystallographic protomers (Pabo & Lewis, 1982; Jordan & Pabo, 1988). It is likely that the Raman perturbations reflect a change induced by the engineered disulfide in the structure or dynamics of the dimer contact. The relevance of these features to protein–DNA recognition was tested by comparing the Raman spectra of the wild-type and mutant complexes. Remarkably, those purine vibrational bands perturbed in the wild-type complex are not all perturbed by binding of the mutant protein, implying that specific protein–DNA contacts differ in the two complexes. In addition, a net change in Raman bands reflecting tyrosine hydrogen bonding is observed in the wild-type complex but not in the mutant complex. This feature is presumed to involve the Y22 phenolic OH contact with the phosphate of thymine T1, as seen in the cocrystal structure (Jordan & Pabo, 1988). These findings suggest that the engineered disulfide stabilizes a dimer that differs in some way from the wild-type dimer and cannot optimize those dimer-related protein–DNA interactions required for full activity. We propose that flexibility in the dimer contact and its connection to the remainder of the domain (the loop between helices 4 and 5) is involved in optimizing specific local interactions between the λ repressor and operator in an induced-fit mechanism.

Conclusions

Regulation of protein function is often accomplished by the allosteric control of subunit orientation. In this paper we have described comparative laser Raman spectroscopic studies of wild-type and mutant forms of the operator-binding domain of the λ repressor (residues 1–102). Interactions in solution of (i) the wild-type and mutant repressors with a single operator DNA site and of (ii) a repressor variant with two distinct operators have been analyzed. This system provides a general model for investigating nonlocal effects of changes in subunit orientation on protein–DNA recognition.

The present study is based upon the design and construction of a mutant repressor containing an engineered disulfide bond (Pabo & Suchanek, 1986; Sauer et al., 1986) and has led to the following conclusions: (1) Although the mutation site (Y88C) is located within helix 5, no major change is observed by Raman spectroscopy in the secondary structure of the repressor domain. (2) Whereas the Raman spectrum of the wild-type domain is concentration dependent, reflecting the formation of a noncovalent dimer (Thomas et al., 1986), the spectrum of the mutant domain is not affected by protein concentration. This result is in accordance with the disulfide linkage of the mutant dimer, which is observed in the spectrum of the mutant domain as a disulfide-specific Raman band centered at 529 cm^{-1}. Interestingly, this vibrational frequency indicates that disulfide bonds of the mutant dimer generally lack configurational symmetry (i.e., the g/g/t rotamer is the most populated CC–S–S–CC conformation, although substantial g/g/g and t/g/t conformations may coexist). Absence of rigorous 2-fold symmetry has previously been described in the refined crystal structures of the wild-type domain (Pabo & Lewis, 1982) and its operator complex (Jordan & Pabo, 1988). (3) When the N-terminal domain binds the operator site O_L1, changes are observed in the Raman signatures of both DNA and protein. These changes indicate significant perturbations to the local B-form conformation of DNA in the complex, as described elsewhere (Benevides et al., 1991), and provide direct evidence for similarity of crystal and solution structures of the repressor–operator complex (Jordan & Pabo, 1988). Remarkably, the wild-type and Y88C domains do not generate identical perturbations to O_L1 DNA conformation upon binding. Differences in the pattern of interaction exhibited by wild-type and mutant repressors suggest that flexibility at the dimer interface is an important requirement for binding. Accordingly, we propose that the intersubunit disulfide bond imposes configurational constraints at the helix 5/helix 5′ interface that disallow induced fit of a quaternary structure required for optimal operator binding. (4) The major changes in the protein Raman spectrum with operator binding are confined to bands that report side chain interactions. These interactions include a change in hydrogen-bonding state of the phenolic OH group of Y22 (deduced to donate a hydrogen bond to an O_L1 phosphate oxygen of thymine 1) and in configurations of side-chain Cα–Cβ bonds (deduced to occur primarily at the protein–DNA and protein–protein interfaces).

The present study of an engineered disulfide bond in the λ repressor demonstrates the general utility of laser Raman spectroscopy in characterizing local and nonlocal effects of site-directed mutations. Future studies of the λ repressor–operator system will focus on the effects of additional mutations in key regions of the protein, including the "recognition" helix and N-terminal arm. We anticipate that these studies of a representative helix–turn–helix protein will provide a prototype for the Raman study of other conserved motifs of protein–DNA recognition.

Acknowledgments

We thank Prof. M. Karplus (Harvard University) and Prof. R. T. Sauer (Massachusetts Institute of Technology) for advice and support during early stages of this work (M.A.W.) and Prof. C. O. Pabo (Johns Hopkins University) for refined crystal coordinates and helpful discussions. We also thank A. Jeitler-Nilsson and K. Hehir for help with protein purification and Dr. D. T. Nguyen for the computer graphics.

References

Aggarwal, A. K., Rodgers, D. W., Drottar, M., Ptashne, M., & Harrison, S. C. (1988) *Science 242*, 899–907.

Bellamy, L. J. (1980) *The Infrared Spectra of Complex Molecules, Advances in Infrared Group Frequencies*, Vol.

2, Second ed., Chapman and Hall, New York.
Benevides, J. M., Wang, A. H.-J., van der Marel, G. A., van Boom, J. H., Rich, A., & Thomas, G. J., Jr. (1984) *Nucleic Acids Res. 12*, 5913–5925.
Benevides, J. M., Wang, A. H.-J., Rich, A., Kyogoku, Y., van der Marel, G. A., van Boom, J. H., & Thomas, G. J., Jr. (1986) *Biochemistry 25*, 41–50.
Benevides, J. M., Wang, A. H.-J., van der Marel, G. A., van Boom, J. H., & Thomas, G. J., Jr. (1988) *Biochemistry 27*, 931–938.
Benevides, J. M., Weiss, M. A., & Thomas, G. J., Jr. (1991) *Biochemistry 30* (in press).
Brennan, R. G., Roderick, S. L., Takeda, Y., & Matthews, B. W. (1990) *Proc. Natl. Acad. Sci. U.S.A. 87*, 8165–8169.
Harrison, S. C., & Aggarwal, A. K. (1990) *Annu. Rev. Biochem. 59*, 933–969.
Hartman, K. A., Lord, R. C., & Thomas, G. J., Jr. (1973) in *Physico-Chemical Properties of Nucleic Acids* (Duchesne, J., Ed.) Vol. 2, pp 1–89, Academic Press, New York.
Hecht, M. H., Nelson, H. C. M., & Sauer, R. T. (1980) *Proc. Natl. Acad. Sci. U.S.A. 80*, 2676–2680.
Hochschild, A., Irwin, N., & Ptashne, M. (1983) *Cell 32*, 319–325.
Jordan, S. R., & Pabo, C. O. (1988) *Science 242*, 893–899.
Krimm, S. (1987) in *Biological Applications of Raman Spectroscopy* (Spiro, T. G., Ed.) Vol. 1, pp 1–45, Wiley, New York.
Lim, W. A., & Sauer, R. T. (1989) *Nature 339*, 31–36.
Lord, R. C., & Thomas, G. J., Jr. (1967) *Spectrochim. Acta 23A*, 2551–2591.
Mondragon, A., Wolberger, C., & Harrison, S. C. (1989a) *J. Mol. Biol. 205*, 179–188.
Mondragon, A., Subbiah, S., Almo, S. C., Drottar, M., & Harrison, S. C. (1989b) *J. Mol. Biol. 205*, 189–200.
Nishimura, Y., Tsuboi, M., Sato, T., & Aoki, K. (1986) *J. Mol. Struct. 146*, 123–153.
Pabo, C. O., & Lewis, M. (1982) *Nature 298*, 443–447.
Pabo, C. O., & Suchanek, E. G. (1986) *Biochemistry 25*, 5987–5991.
Prescott, B., Steinmetz, W., & Thomas, G. J., Jr. (1984) *Biopolymers 23*, 235–256.
Reidhaar-Olson, J. F., & Sauer, R. T. (1988) *Science 241*, 53–57.
Sauer, R. T., Pabo, C. O., Meyer, B. J., Ptashne, M., & Backman, K. D. (1979) *Nature 279*, 396–400.
Sauer, R. T., Hehir, K., Stearman, R. S., Weiss, M. A., Jeitler-Nilsson, A., Suchanek, E. G., & Pabo, C. O. (1986) *Biochemistry 25*, 5992–5998.
Siamwiza, M. N., Lord, R. C., Chen, M. C., Takamatsu, T., Harada, I., Matsuura, H., & Shimanouchi, T. (1975) *Biochemistry 14*, 4870–4876.
Small, E. W., & Peticolas, W. L. (1971) *Biopolymers 10*, 69–88.
Spiro, T. G., Ed. (1987) *Biological Applications of Raman Spectroscopy, Raman Spectra and the Conformations of Biological Macromolecules*, Vol. 1, Wiley, New York.
Steitz, T. A. (1990) *Q. Rev. Biophys. 23*, 205–280.
Sugeta, H., Go, A. and Miyazawa, T. (1973) *Bull. Chem. Soc. Jpn 46*, 3407–3411.
Thomas, G. J., Jr., & Wang, A. H.-J. (1988) *Nucleic Acids Mol. Biol. 2*, 1–30.
Thomas, G. J., Jr., Prescott, B., Benevides, J. M., & Weiss, M. A. (1986) *Biochemistry 25*, 6768–6778.
Weiss, M. A., Redfield, A. G., & Griffey, R. H. (1986) *Proc. Natl. Acad. Sci. U.S.A. 83*, 1325–1329.
Weiss, M. A., Karplus, M., & Sauer, R. T. (1987a) *Biochemistry 26*, 890–896.
Weiss, M. A., Pabo, C. O., Karplus, M., & Sauer, R. T. (1987b) *Biochemistry 26*, 897–904.
Wolberger, C., Dong, Y. Ptashne, M., & Harrison, S. C. (1988) *Nature 335*, 789–795.